Signal Processing of Sensor Node Data for Vehicle Detection

Jiagen (Jason) Ding, Sing-Yiu Cheung, Chin-Woo Tan and Pravin Varaiya, *Fellow, IEEE*

Abstract— **In this paper we describe the experimental work and present an algorithm for vehicle detection using sensor node data. Both acoustic and magnetic signals are processed for vehicle detection. We propose a real-time vehicle detection algorithm called the Adaptive Threshold algorithm (ATA). This adaptive algorithm first computes the time-domain energy distribution curve and then slices the energy curve using a threshold updated adaptively by some decision states. Finally, the hard decision results from threshold slicing are passed to a finite-state machine, which makes the final vehicle detection decision. Real-time tests and offline simulations both demonstrate that the proposed algorithm is effective.**

I. Introduction

The idea of deploying sensors to *monitor/measure* the behaviour of a system is not novel; however, some of the technological and economic issues remain challenging. In particular, many issues need to be considered for the price one is willing to pay for collecting information and making system improvement. For example, can we collect the data we want with only wired sensors? Wireless sensors offer the flexibility advantage, but just like any portable device, the limit of the energy source is always a concern. Can we deploy a network of sensors so that we have a high density and fidelity of instrumentation? A high density of sensors is an obvious benefit, but it also means more cost. In other words, is large-scale deployment economically feasible? All these issues, nonetheless, can be categorised into three inter-related categories: *cost*, *benefit*, and *technological limitation*. These three issues will dictate the choice of the sensing device for applications such as vehicle detection.

A vehicle detection system has four main components: a sensor to sense the signals generated by vehicles, a processor to process the sensed data, a communication unit to transfer the processed data to the base station for further processing, and an energy source. Conventional vehicle detection technologies, such as inductive loop detectors, are not suitable for large-scale deployment because they are usually intrusive and disruptive to traffic, resulting in high installation and maintenance costs. By lowering the cost barriers and reducing the complexity of collecting information from the physical world, *wireless* sensor technology frees sensors to go where cost and practicality have kept them from going in the past. Also with recent advances in microelectronics and MEMS technology, all of the four main components of a vehicle detection system can now be integrated into a tiny single device called a *sensor node*. Each of these sensor nodes is called a *Mote*. In the future, a vehicle detection system can be a network of low-cost sensor nodes interconnected as an ad hoc network via wireless communication. This could be deployed with low maintenance costs by controlling the power consumption of the energy source for transmission and reception of data packets [8]. One such sensor node, shown in Figure 1, is developed under the Smart Dust research project conducted at the Department of Electrical Engineering and Computer Sciences, University of California, Berkeley [1, 2]. These wireless sensor nodes are battery powered and are expected to have a lifetime of couple of years. Thus, it makes sense that each sensor node processes the sensor data locally and sends only the vehicle detection results back to the base station (or gateway sensor node). This will reduce the sensor network traffic and achieve a longer lifetime of operation. In what follows, we first review some of the current signal processing techniques for vehicle detection.

Various signal-processing algorithms for vehicle detection have been proposed for vehicle detection [3,4,5]. These algorithms are for detecting vehicle acoustic signals, and the analysis are based in three domains: time, frequency, and time-frequency domains. Acoustic signal

Manuscript received April 1, 2004. This work was supported in part by the Division of Research and Innovation, U. S. California Department of Transportation, under Task Orders 4153 and 4224.

J. Ding was a Ph.D. student with the Dept. of Electrical Engineering and Computer Sciences, and the Dept. of Mechanical Engineering, University of California, Berkeley, CA 94720, USA. He is now with the General Electric Research Center, Niskayuna, NY 12345, USA. (phone: (518) 387-4020; e-mail: ding@ research.ge.com).

S.-Y. Cheung is a Ph.D. student with the Department of Mechanical Engineering, University of California, Berkeley, CA 94720, USA. (e-mail: sing@uclink4. berkeley.edu).

C.-W. Tan is a researcher with the California PATH program, U. C. Berkeley Richmond Field Station, Richmond, CA 94804, USA. (e-mail: tan@eecs.berkeley.edu).

P. Varaiya is a Professor with the Department of Electrical Engineering and Computer Sciences, University of California, Berkeley, CA 94720, USA. (e-mail: varaiya@eecs.berkeley.edu)

processing in time domain, such as beam-forming [3], is a natural approach, but not an optimal one due to the complexity of the environment, i.e., the time domain signatures of acoustic signals can be hampered by noise from other moving vehicles, Doppler effects, wind, and so on. The frequency domain signal processing algorithms are focused on the frequency range from 20 to 200Hz where vehicle acoustic signals are generated from two main sources: the engine and the propulsion gear. The harmonic line association (HLA) algorithm was developed in [4, 5] based on these characteristics. However, since vehicle acoustic signals are non-stationary and wide-band, it is very difficult to pick peaks in the frequency spectrum. So other approaches in time-frequency domain, such as wavelet-based algorithms, were developed as well [5]. Wavelet-based algorithms are not suitable for real-time vehicle detection for they tendto require intensive computation and samples from a long period of time. The simple algorithm for vehicle detection using magnetometer data is a fixed threshold detection algorithm [7]. This fixed threshold algorithm is not robust because the magnetic signal amplitude changes with the size of the vehicle. In this paper we propose an *adaptive threshold algorithm* (ATA) suitable for real-time vehicle detection applications. The ATA is a time-domain energy- distribution-based alogrithm. This algorithm first computes the time-domain energy distribution curve and then slices the energy distribution curve using a threshold updated adaptively by some decision states. Finally, the hard decision results from threshold slicing are passed to a finite state machine, which makes the vehicle detection decision. It is noted that the ATA is an energy-based algorithm with an adaptive threshold, which makes it robust and insensitive to environmental noises. The ATA is also a real-time vehicle detecion algorithm.

Figure 1: Sensor nodes, also known as Motes

The rest of this paper is organized as follows: Section II discusses the type of wireless sensor node (Mote) used for vehicle detection. Section III develops the Adaptive Threshold Algorithm (ATA) for vehicle detection. Section IV demonstrates the simulation and experimental results of ATA for vehicle detection. Some concluding remarks are given section V.

II. SENSOR NODES

The sensor nodes (Motes) used in our vehicle detection experiments are jointly developed by the EECS Department at UC Berkeley and Intel [1]. In a Mote, the essential components for vehicle detection (processor, memory, sensor and radio) are integrated together with a form factor as small as a quarter coin (see Figure 1). The Mote consists of two major components: a motherboard and a sensor board. The sensor board includes both acoustic and magnetic sensors, both used in our vehicle detection experiments.

The basic operating principles of acoustic sensors and magnetometers will be presented next.

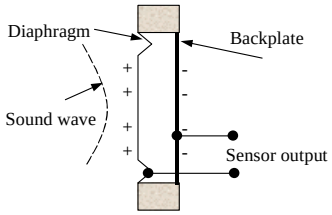

Figure 2: Schematic of a condenser microphone

A. Acoustic Sensors

The acoustic sensor in the Mote is the Panasonic WM-62A microphone, which is a condenser type microphone. The schematic for a typical condenser acoustic sensor is shown in Figure 2. It includes a stretched metal diaphragm that forms one plate of a capacitor. A metal disk placed close to the diaphragm acts as a back-plate. A stable DC voltage is applied to the plates through a high resistance to keep electrical charges on the plates. When a sound field excites the diaphragm, the capacitance between the two plates varies according to the variation in the sound pressure. The change in the capacitance generates an AC output voltage proportional to the sound pressure. Figure 3 shows a typical measured vehicle acoustic signal waveform.

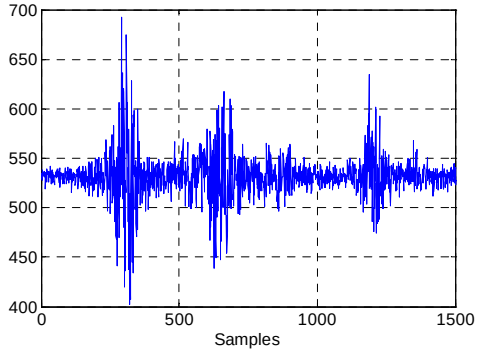

Figure 3: A typical measured vehicle acoustic signal

B. Magnetic Sensors

The magnetic sensor in the Mote is the Honeywell HMC1002 magnetometer, which is a magnetoresistive sensor. The anisotropic magnetoresistive (AMR) sensor has

a wide range for sensing the Earth's magnetic field and provides both the strength and direction of the Earth field [6]. Figure 4 shows the magnetoresistive effect of Permalloy. The resistance of Permalloy is a function of the angle (θ) between the bias current and the magnetization vector ($\vec{M}$). The applied magnetic field changes the direction of the magnetization vector and thus changes the resistance, which is used for magnetic field sensing. The AMR sensor is made of a nickel-iron (Permalloy) thin film deposited on a silicon wafer and patterned as resistive strips. Typically, four of these resistive strips are connected in a Wheatstone bridge configuration so that both magnitude and direction of a field along a single axis can be measured. The key benefit of AMR sensors is that they can be bulk manufactured on silicon wafers and mounted into commercial integrated circuit packages.

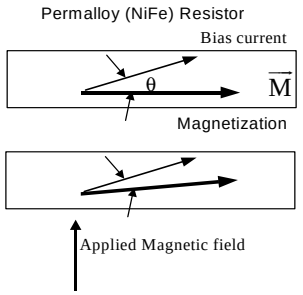

Figure 4: Permalloy magnetoresistive effect

Figure 5 shows a typical change of Earth magnetic field along one axis when a vehicle passes over the AMR sensor.

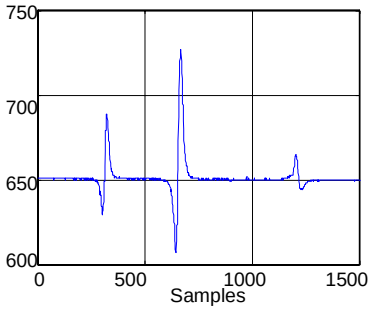

Figure 5: A typical measured vehicle magnetic signal

III. ADAPTIVE THRESHOLD ALGORITHM

This section presents the adaptive threshold detection algorithm. The algorithm consists of computation of energy distribution curve, filtering of energy signal, state machine detector and threshold adaptation. The block diagram of the adaptive threshold detection algorithm is shown in Figure 6. As shown in the figure, Square&Decimator, Filtering, Adaptive Threshold and Decision correspond to energy distribution curve computation, energy signal filtering, threshold adaptation and state machine detector, respectively.

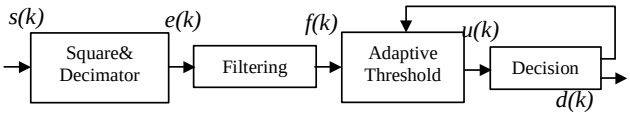

Figure 6: Block diagram of adaptive threshold detection

A. Energy Distribution Computation

The original measured acoustic or magnet signal may need to be first filtered by a band-pass filter to remove environmental noise (not shown in Fig. 6), such as the wind noise for acoustic signal. The band-pass filter output *s(k)* is squared and may be decimated, which results in energy signal *e(k)*. This energy signal *e(k)* is related to the *s(k)* by:

$$e(k) = [s(Nk)]^2 \quad (1)$$

where *N* is the decimating rate.

B. Smoothing of Acoustic Energy Signal

The energy signal, *e(k)*, could be very jerky and a low-pass filter is used to smooth it for later detection. In our ATA algorithm, the low-pass smooth filter is chosen to be low-pass FIR filter, which has the advantages of linear phase and inherent stability. The key design parameters for low-pass FIR filters are the -3dB cutoff frequency (ω_p), the stop band frequency (ω_s) and the stop band attenuation gain. The smoothed energy signal *f(k)* is passed to the Adaptive Threshold block to make the hard decision.

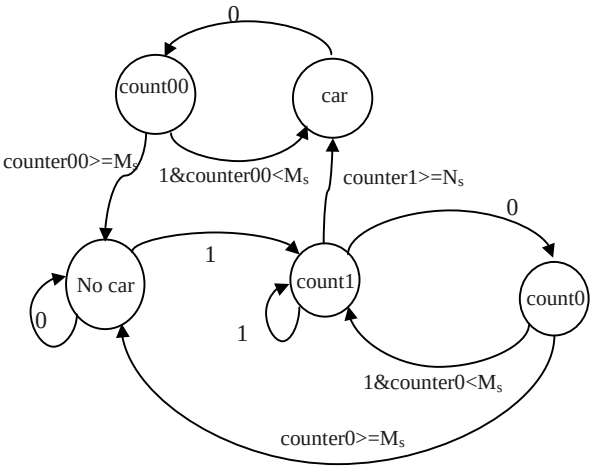

Figure 7: State diagram for state machine detector

C. Adaptive Threshold Decision

The hard decision produces an output $u(k) = 1$ if the input sample $f(k)$ is larger than the current detection threshold $T(k)$. Otherwise, the hard decision will produce an output $u(k) = 0$. The value of the threshold $T(k)$ is adaptively updated, which will be addressed in next. First, the moving average of the energy signal is computed as:

$$MA(k) = \frac{f(k) + f(k-1) + \ldots + f(k-M+1)}{M} \quad (2)$$

where MA denotes the moving average of the smoothed energy signal $f(k)$ and M is the number of moving average samples. The adaptive threshold $T(k)$ is updated as follows:

If the current decision state is at "car" state

$$T(k) = \alpha MA(k - M_d) + T_{offset}$$

else

$$T(k) = \beta MA(k-Md) + T_{offset} \quad (3)$$

where α *(<1)* and β *(* >1) are two parameters for adjusting the moving average, M_d is an integer for delaying the moving average, and T_{offset} is a constant which sets the minimum threshold. It is noted that the adaptive threshold is the delayed moving average of the past energy levels which is scaled corresponding to the decision states. We next discuss how the decision states are computed.

D. State Machine Detector

Figure 7 shows the state diagram for the state machine corresponding to the decision block shown in Figure 6. The state machine consists of :

State(x(k)) : { nocar, car, count1, count0, count00 }

Input(u(k)) : { 1, 0 }

Output(d(k)) : { car, nocar }

The input in the state machine is defined as:

u(k) = 1 if f(k)>T(k)

= 0 otherwise

There is a counter for each state of *{count1, count0, count00}* and the counter at each state resets whenever the state machine jumps back from other states.

The state machine starts at the state *no car* and stays at this state if the input $u(k)$ remains 0. The state machine jumps from state *no car* to state *count1* if the input is 1 ($u(k) = 1$). When the state machine enters state *count1*, the counter counts up and the state machine stays at this state if the input $u(k)$ is 1 and the previous counter value is less than N_s. The state machine jumps from c*ount1* to *count0* if the input is 0 and to car if the input is 1 and the previous counter value is not less than N_s. When the state machine enters state *count0*, the counter at this state counts up and the state machine stays at this state if the input $u(k)$ is 0 and the previous counter value is less than M_s. The state machines jumps from *count0* to *count1* if the input $u(k)$ is 1 and to state *no car* if the input is zero and the previous counter value is not less than M_s**.** When the state machine enters state *car*, it will stays at this state if the input is 1 and jumps to *count00* if the input is 0. When the state machine enters state *count00*, the counter at this state counts up and the state machine stays at this state if the input is 0 and the previous counter value is less than M_s. The state machine jumps from *count00* to count *car* if the input is 1 and to *no car* if the input is zero and the previous counter value is not less than Ms. One vehicle is detected when the state machine jumps from state *count1* to state *car*.

It is noted that the counter at the states *{count1, count0, count00}* and parameters M_s *and* N_s introduce hysteresis in the detection, which will make the algorithm more robust to the short burst errors in the hard decision.

IV. Simulation and Online Experiment

A. Acoustic Signal Vehicle Detection

This section will demonstrate the ATA algorithm by simulation and experiments. The algorithm is prototyped in a laptop-based system as shown in Figure 8. Real-time tests and offline simulation results are both presented for this prototype system. Secondly, only the offline algorithm simulation is presented for the acoustic signals measured by the Mote because the limited computing resource in the Mote system makes real-time tests difficult.

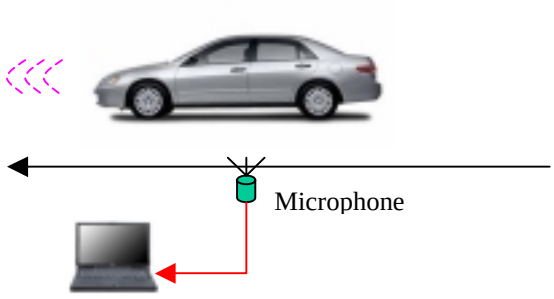

Figure 8: Laptop based acoustic vehicle detection

Figure 9 shows some real-time vehicle detection results of the adaptive threshold algorithm. The decision results with 1's at around 1.8, 4, 6.8, 8.2, 10, 12, and 14 seconds represent vehicle existence at those time instants. The states 0,1,2,3 and 4 in the state transition traces correspond to states no car, car, count0, count1 and count00, respectively. It is noted that the Adaptive Threshold Algorithm gives the correct real-time detection. Figure 10 shows a snap shot of a long-time ATA simulation result. In this figure, the blue line corresponds to the energy distribution curve and the red line corresponds the threshold traces.

Next we study the effect of parameter choices on the performance of the ATA acoustic vehicle detection. The key parameters are the counter limits (M_s and N_s) in Figure 7 and the threshold adjustment coefficients (α and β) in

Equation 3.

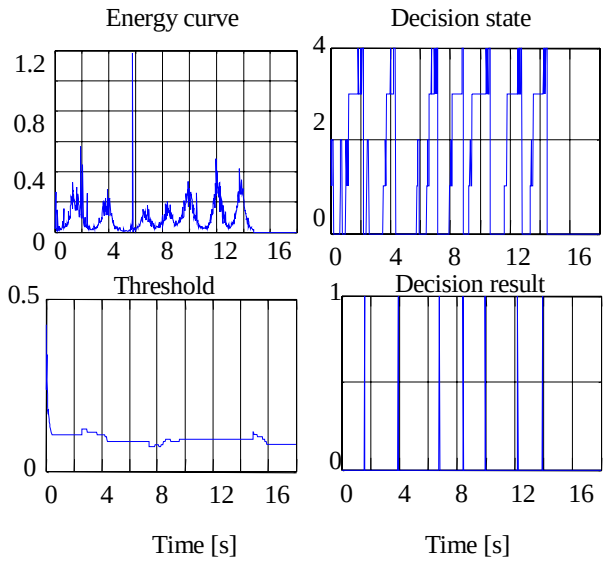

Figure 9: ATA acoustic vehicle detection

Table 1 summarizes the effect of M_s and N_s on the ATA acoustic vehicle detection results with α=0.7, β=1.5 and the threshold offset T_{offset} =2e-5. The smoothing filter is just a 40point moving average and M_d is chosen to be 20. It is noted that large M_s and N_s lead to better robustness but may miss detecting high speed vehicles. M_s *and* N_s should be chosen by trading off the algorithm robustness and the speed range of detectable vehicle. A small N_s could result in overcount due to a short burst of 1's caused by noise while a large N_s may result in the missed detection of fast vehicles. On the other hand, a small M_s could cause overcount due to noise while a large M_s may have poor resolution when two vehicles are very close to each other.

Table 1: The effect of M_s *and* N_s on ATA

(N_s,M_s)	Ground truth (# of vehicles)	Detection result (# of vehicles)
(10,10)	63	62
(10,15)	63	64
(10,20)	63	62
(20,10)	63	60
(15,10)	63	62
(10,10)	63	63
(6, 10)	63	70

Table 2 summarizes the effect of α and β on the ATA performance with (N_s, M_s) = (10, 10) and the threshold offset T_{offset}=2e-5. The smoothing filter is just the 40-point moving average and M_d is chosen to be 20. It is noted that the performance is quite robust to the choices of α and β.

B. Mote Acoustic Vehicle Detection

The sampling frequency for the acoustic sensor in Mote system is 256 Hz, which is much lower than the laptop-based prototype system. The algorithm block diagram is the same as the laptop system. Since the Mote system has limited computing resources, the algorithm is not implemented in the Mote but is simulated offline with the measured acoustic signal from the Mote. Figure 10 shows the ATA simulation results for the Mote system. In Figure 11, the left plot is the original acoustic waveform measured by the Mote and the right plot is the energy curve and the adaptive threshold trace. It is noted that ATA detected three vehicles correctly.

Table 2: The effect of (α,β) on ATA

(α,β)	Ground truth (# of vehicles)	Detection result (# of vehicles)
(0.7,1.8)	63	58
(0.7,1.5)	63	62
(0.7,1.3)	63	66
(0.8,1.5)	63	66
(1.0,1.5)	63	63

C. Magnetic Signal Vehicle Detection

The threshold slicing algorithm had been implemented on the Smart Dust [1] [2] MICA sensor mote. The following will present the ATA magnetic vehicle detection results.

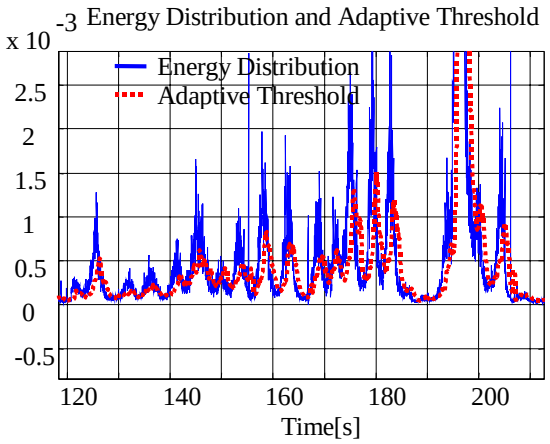

Figure 10: Long time simulation of ATA detection

Figure 12 shows the ATA magnetic vehicle detection. The left plot shows the magnetic signal waveform with 4 vehicles passing over the Mote with a magetometer. The sampling frequency for magentic signals is 64 Hz. The same ATA was implemented as for acoustic vehicle detection via Motes. All the four vehicles are correctly detected.

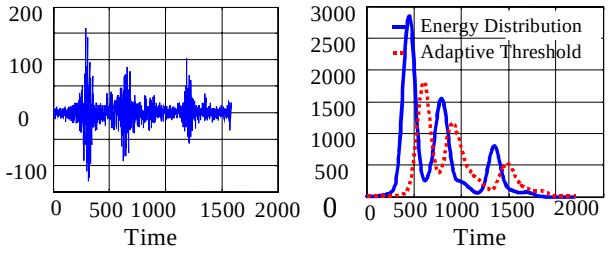

Figure 11: ATA acoustic detection using the Mote

V. CONCLUSION

This paper discusses an innovative real-time vehicle detection algorithm: the Adaptive Threshold. Real-time tests and offline simulations have demonstrated that the algorithm is effective for processing both acoustic and magnetic signals for vehicle detection. The effect of tuning several key parameters of the ATA were also presented. The signal processing of the magnetic signals using the threshold algorithm results in 0-1 pulses. From the widths of the pulses, we can estimate the vehicle speed if the length of the vehicle is known. Our future research work will involves speed estimation using multiple Motes.

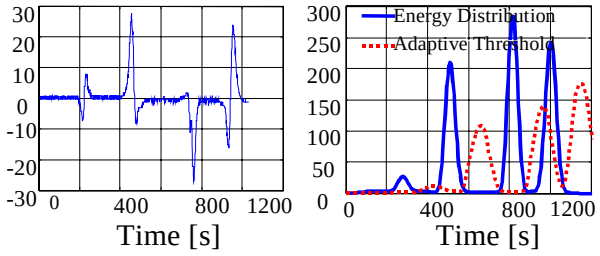

Figure 12: ATA magnetic vehicle detection using the Mote

ACKNOWLEDGMENT

This work was supported by the Division of Research and Initiative (DRI), U. S. California Department of Transportation under Task Orders 4153 and 4224.

REFERENCES

[1] TinyOS, A component-based OS for the networked sensor regime, http://webs.cs.berkeley.edu/tos/.
[2] Crossbow, Manufacturer of Smart-Dust, http://www.xbow.com/
[3] Russell Braunling, Randy M. Jensen, and Michael A. Gallo, "Acoustic target detection, tracking, classification, and location in a multiple target environment," in *Peace and Wartime Applications and Technical Issues for Unattended Ground Sensor*s, 1997, vol. 3081, pp. 57–66.
[4] George Succi and Torstein K. Pedersen, "Acoustic target tracking and target identification - recent results," in *Unattended Ground Sensor Technologies and Application*s, Orlando, Florida, April 1999, SPIE, vol. 3713, pp. 10–21
[5] Howard C. Choe, Robert E. Karlsen, Grant R. Gerhert, and Thomas Meitzler, "Wavelet-based ground vehicle recognition using acoustic signal," in *Wavelet Applications III*, 1996, vol. 2762, pp. 434–445.
[6] S. Coleri, M.Ergen, and T.J. Koo, "Lifetime analysis of a sensor network with hybrid automata modeling", Processings of ACM International Workshop on Wireless Sensor Networks and Applications (Atlanta, GA), Sept. 2002.
[7] Michael J. Caruso, Lucky S. Withanawasam, "Vehicle Detection and Compass Applications using AMR Magnetic Sensors", Honeywell, SSEC, 12001 State Highway 55, Plymouth, MN USA 55441 http://www.ssec.honeywell.com
[8] S. Coleri, "PEDAMACS: Power Efficient and Delay Aware Medium Access Protocol for Sensor Networks**"** Master Thesis, University of California Berkeley, December 2002.